HEFAT 2012
9th International Conference on Heat Transfer, Fluid Mechanics and Thermodynamics
16-18 July 2012
Malta

SOLID/LIQUID DENSITY DIFFERENCES AND THE INITIAL STAGES OF PHASE CHANGE IN THE PRESENCE OF NATURAL CONVECTION

Vynnycky M.*
Mathematics Applications Consortium for Science and Industry (MACSI)
Department of Mathematics and Statistics
University of Limerick
Limerick
Ireland
E-mail: michael.vynnycky@ul.ie

ABSTRACT The solidification of a pure liquid phase-change material in the presence of natural convection is a commonly recurring problem in natural science and technology. The numerical solution of this Stefan problem is made difficult by the fact that there is initially no solid phase; hence, the classical 1D Neumann similarity solution is often used for the purposes of initiating a computation. However, if the solid and liquid phases have different densities at the solidification temperature, this solution is not valid. This paper considers the limit of the coupled heat and momentum equations for small times, and finds that it is not possible to solve the corresponding problem, when the densities are different, without introducing a singularity into the liquid velocity and pressure. The solution to a non-classical Stefan problem, where cooling is due to a constant heat flux, is also considered, and is found to be free from such singularities.

INTRODUCTION

Buoyancy-driven flows with coupled solid–liquid phase change occur in a broad range of scientific and engineering fields; often cited examples are those in the solidification and melting phenomena encountered in metallurgical processes, latent heat thermal energy storage, oceanography, food processing and nuclear reactor safety. Consequently, there is also a focus on the development of numerical methods to solve such problems.

A particular difficulty is the fact that initially only one phase is present; in this paper, we will only consider solidification, so that it is only the liquid phase that is initially present. Often, when applying a front-tracking numerical method, a small amount of solid phase of uniform thickness is assumed to be present in order to initiate a numerical computation [1-3]; in tandem, it is necessary to prescribe appropriate initial velocity and temperature fields. For the velocity field, it is convenient just to assume that the liquid is stationary. For the temperature, the simplest approach is, having already assumed a solid layer of uniform thickness, to use the Neumann solution to the classical 1D Stefan problem. This approach is adequate if, at the melting temperature, the density of the liquid phase is equal to the density of the solid phase. Otherwise, the density difference will induce a velocity in the liquid, rendering the assumptions on the initial velocity and temperature fields incompatible with each other; indeed, it is only very recently that any progress has been made with this scenario [4], although in the context of heat transfer alone. The purpose of this paper is to derive appropriate starting conditions for a computation in which solid and liquid densities are different. The idea is similar to that used in several recent solidification problems [5,6], albeit now with the added complexity of a non-zero velocity field in the liquid phase. It is also worth noting that although using another numerical method, such as the enthalpy formulation on a fixed grid, would not require such attention to detail as regards the start of solidification, it is also likely that such methods would not have the accuracy required to resolve the motion of the solidification front correctly, and to reproduce the interfacial patterns that are observed experimentally [7-9].

The layout of the paper is as follows. First, model equations are formulated, and then nondimensionalized. Their behaviour is then considered in the limit of small time; this leads to a system of similarity ordinary equations that are solved semi-analytically. The mathematical singularities associated with these solutions are discussed, and an alternative formulation is proposed, which is then shown to remove these singularities.

NOMENCLATURE

Bi	[-]	Biot number, $h_0\mathfrak{h}/k_l$
c_{pl}	[J/kgK]	liquid specific heat capacity
c_{ps}	[J/kgK]	solid specific heat capacity
f	[-]	function defined in equation (64)
F_l	[-]	function given by equation (62)
F_s	[-]	function given by equation (58)
g	[m/s^2]	gravitational acceleration
h	[m]	location of the liquid surface
h_0	[m]	initial liquid height
H	[-]	dimensionless liquid height
k_l	[W/mK]	liquid thermal conductivity
k_s	[W/mK]	solid thermal conductivity
$\mathbf{n}_h$	[-]	unit vector normal to $y = h(x,t)$
$\mathbf{n}_s$	[-]	unit vector normal to $y = s(x,t)$
p	[Pa]	pressure
$[p]$	[Pa]	pressure scale, $\mu k_l/h_0^2\rho_{l0}c_{pl}$
P	[-]	dimensionless pressure
Pr	[-]	Prandtl number
Ra	[-]	Rayleigh number
s	[m]	location of the solidification front
S	[-]	dimensionless location of the solidification front
St	[-]	Stefan number
t	[s]	time
$[t]$	[s]	time scale, $\rho_{l0}c_{pl}h_0^2/k_l$
$\mathbf{t}_h$	[-]	unit vector tangential to $y = h(x,t)$
$\mathbf{t}_s$	[-]	unit vector tangential to $y = s(x,t)$
T_l	[K]	liquid temperature
T_s	[K]	solid temperature
T_{cold}	[K]	cooling temperature
T_{hot}	[K]	initial liquid temperature
T_{melt}	[K]	solidification temperature
T_0	[K]	reference temperature
u	[m/s]	velocity in x-direction
$[u]$	[m/s]	velocity scale, $k_l/h_0\rho_{l0}c_{pl}$
v	[m/s]	velocity in y-direction
U	[-]	dimensionless velocity in X-direction
V	[-]	dimensionless velocity in Y-direction
V_0	[-]	dimensionless constant given in equation (57)
x	[m]	horizontal coordinate
X	[-]	dimensionless horizontal coordinate
y	[m]	vertical coordinate
Y	[-]	dimensionless vertical coordinate

Special characters

$\mathfrak{h}$	[W/m^{2}K]	heat transfer coefficient
α	[1/K]	thermal expansion coefficient
ΔH_f	[J/kg]	latent heat of fusion
η	[-]	dimensionless similarity variable
θ	[-]	dimensionless temperature
θ_{cold}	[-]	dimensionless cooling temperature
κ	[-]	dimensionless constant, κ_l/κ_s
κ_l	[m^2/s]	liquid thermal diffusivity, $k_l/c_{pl}\rho_l(T_{melt})$
κ_s	[m^2/s]	solid thermal diffusivity, $k_s/c_{ps}\rho_s(T_{melt})$
λ	[-]	dimensionless variable in equation (64)
μ	[kg/ms]	liquid dynamic viscosity
ν	[-]	dimensionless constant given in equation (57)
Π	[-]	dimensionless function of η and τ
ρ	[-]	$\rho_s(T_{melt})/\rho_l(T_{melt})$
ρ_l	[kg/m^3]	density of liquid phase
ρ_{l0}	[kg/m^3]	reference liquid density
ρ_s	[kg/m^3]	density of solid phase
τ	[-]	dimensionless time
τ_m	[-]	dimensionless time until the start of solidification

MATHEMATICAL FORMULATION

To fix ideas, this paper considers the freezing from below of a fluid with freezing temperature T_{melt}, initial height h_0 and initial temperature T_{hot}, where $T_{hot} > T_{melt}$. Fig. 1 shows the model geometry.

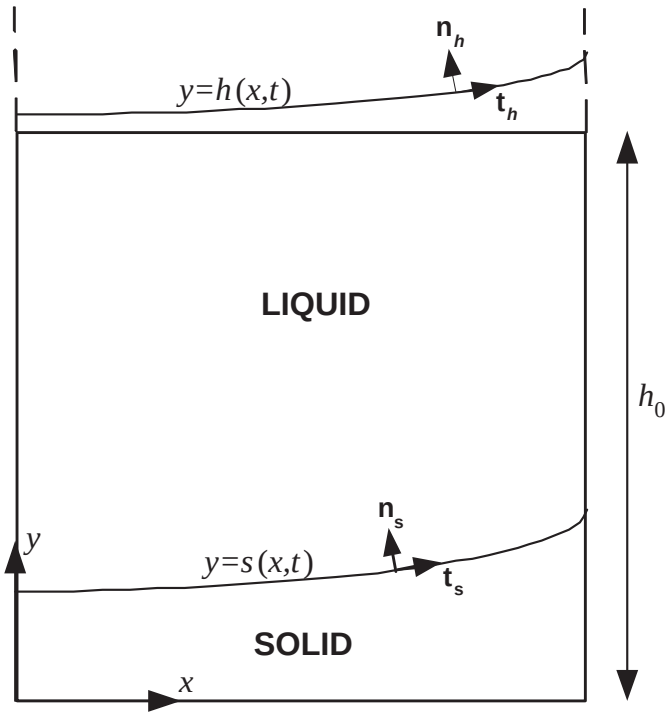

Figure 1: Schematic illustration of the solidification of a fluid from below

Governing equations

For the solid region, we have

$$\rho_s c_{ps}\frac{\partial T}{\partial t} = k_s\left(\frac{\partial^2 T}{\partial x^2} + \frac{\partial^2 T}{\partial y^2}\right), \tag{1}$$

i.e. the equation for transient heat conduction, where ρ_s, c_{ps}, k_s are the density, specific heat capacity and thermal conductivity of the solid phase, respectively. For the liquid phase, we have

$$\frac{\partial \rho_l}{\partial t} + \frac{\partial}{\partial x}(\rho_l u) + \frac{\partial}{\partial y}(\rho_l v) = 0, \tag{2}$$

$$\rho_l\left(\frac{\partial u}{\partial t} + u\frac{\partial u}{\partial x} + v\frac{\partial u}{\partial y}\right) = -\frac{\partial p}{\partial x} + \mu\left(\frac{\partial^2 u}{\partial x^2} + \frac{\partial^2 u}{\partial y^2}\right), \tag{3}$$

$$\rho_l\left(\frac{\partial v}{\partial t} + u\frac{\partial v}{\partial x} + v\frac{\partial v}{\partial y}\right) = -\frac{\partial p}{\partial y} + \mu\left(\frac{\partial^2 v}{\partial x^2} + \frac{\partial^2 v}{\partial y^2}\right) - \rho_l g, \tag{4}$$

$$\rho_l c_{pl}\left(\frac{\partial T_l}{\partial t} + u\frac{\partial T_l}{\partial x} + v\frac{\partial T_l}{\partial y}\right) = k_l\left(\frac{\partial^2 T_l}{\partial x^2} + \frac{\partial^2 T_l}{\partial y^2}\right). \tag{5}$$

For the liquid density, we use

$$\rho_l = \rho_{l0}\left(1 - \alpha\left(T - T_0\right)\right);$$

In addition, μ, c_{pl}, k_l, α are the viscosity, specific heat capacity, thermal conductivity and thermal expansion coefficient of the liquid phase, respectively.

Boundary and initial conditions

At $y = 0$,

$$T = T_{cold}; \tag{6}$$

at $y = h(x,t)$,

$$\nabla T \cdot \mathbf{n}_h = 0, \tag{7}$$

$$\frac{\partial h}{\partial t} = (u, v) \cdot \mathbf{n}_h, \tag{8}$$

$$\mathbf{t}_h \cdot \left(\frac{\partial u}{\partial y} + \frac{\partial v}{\partial x}\right) \cdot \mathbf{n}_h = 0, \tag{9}$$

$$p = 0, \tag{10}$$

where $\mathbf{n}_h$ and $\mathbf{t}_h$ are, respectively, the unit vectors normal and perpendicular to the curves $y = h(x,t)$ and are given by

$$\mathbf{n}_h = (-h_x, 1)/\left(1 + h_x^2\right)^{1/2}, \quad \mathbf{t}_h = (1, h_x)/\left(1 + h_x^2\right)^{1/2}.$$

At $y = s(x,t)$,

$$T = T_{melt}, \tag{11}$$

$$k_s \nabla T \cdot \mathbf{n}_s - k_l \nabla T \cdot \mathbf{n}_s = \rho_s(\Delta H_f)\frac{\partial s}{\partial t}, \tag{12}$$

$$(u, v) \cdot \mathbf{t}_s = 0, \tag{13}$$

$$\rho_l\left(\frac{\partial s}{\partial t} - (u, v) \cdot \mathbf{n}_s\right) = \rho_s \frac{\partial s}{\partial t}, \tag{14}$$

where

$$\mathbf{n}_s = (-s_x, 1)/\left(1 + s_x^2\right)^{1/2}, \quad \mathbf{t}_s = (1, s_x)/\left(1 + s_x^2\right)^{1/2},$$

T_{melt} is the melting/freezing temperature and ΔH_f is the latent heat of fusion.

The initial conditions at $t = 0$ are, for $0 \le y \le h_0$,

$$T = T_{hot}, \quad u = 0, \quad v = 0, \tag{15}$$

and

$$s(x, 0) = 0, \tag{16}$$

$$h(x, 0) = h_0. \tag{17}$$

NONDIMENSIONALIZATION

To nondimensionalize, we set

$$X = \frac{x}{h_0}, \quad Y = \frac{y}{h_0}, \quad S = \frac{s}{h_0}, \quad H = \frac{h}{h_0}, \quad \tau = \frac{t}{[t]},$$

$$\theta = \frac{T - T_{melt}}{T_{hot} - T_{melt}}, \quad U = \frac{u}{[u]}, \quad V = \frac{v}{[u]}, \quad P = \frac{p}{[p]}.$$

Suitable choices for the time, velocity and pressure scales - $[t], [u]$ and $[p]$ respectively - are

$$[t] = \frac{\rho_{l0} c_{pl} h_0^2}{k_l}, \quad [u] = \frac{k_l}{h_0 \rho_{l0} c_{pl}}, \quad [p] = \frac{\mu k_l}{h_0^2 \rho_{l0} c_{pl}}.$$

Governing equations

Equations (1)-(5) become, on applying the Boussinesq approximation,

$$\kappa\frac{\partial \theta}{\partial \tau} = \frac{\partial^2 \theta}{\partial X^2} + \frac{\partial^2 \theta}{\partial Y^2}, \tag{18}$$

$$\frac{\partial U}{\partial X} + \frac{\partial V}{\partial Y} = 0, \tag{19}$$

$$\frac{1}{Pr}\left(\frac{\partial U}{\partial \tau} + U\frac{\partial U}{\partial X} + V\frac{\partial U}{\partial Y}\right) = -\frac{\partial P}{\partial X} + \frac{\partial^2 U}{\partial X^2} + \frac{\partial^2 U}{\partial Y^2}, \tag{20}$$

$$\frac{1}{Pr}\left(\frac{\partial V}{\partial \tau} + U\frac{\partial V}{\partial X} + V\frac{\partial V}{\partial Y}\right) = -\frac{\partial P}{\partial Y} + \frac{\partial^2 V}{\partial X^2} + \frac{\partial^2 V}{\partial Y^2} + Ra\theta, \tag{21}$$

$$\frac{\partial \theta}{\partial \tau} + U\frac{\partial \theta}{\partial X} + V\frac{\partial \theta}{\partial Y} = \frac{\partial^2 \theta}{\partial X^2} + \frac{\partial^2 \theta}{\partial Y^2}, \tag{22}$$

where the Rayleigh number, Ra, and the Prandtl number, Pr, are given, respectively, by

$$Ra = \frac{\rho_{l0}^2 \alpha c_{pl} g\left(T_{hot} - T_{melt}\right) h_0^3}{\mu k_l}, \quad Pr = \frac{\mu c_{pl}}{k_l},$$

and $\kappa = \kappa_l/\kappa_s$, with

$$\kappa_l = \frac{k_l}{c_{pl}\rho_{l0}}, \quad \kappa_s = \frac{k_s}{c_{ps}\rho_s}.$$

Boundary and initial conditions

At $Y = 0$,

$$\theta = \theta_{cold}, \tag{23}$$

where $\theta_{cold} = (T_{cold} - T_{melt}) / (T_{hot} - T_{melt})$; at $Y = H(X, \tau)$,

$$\nabla\theta \cdot \mathbf{n}_h = 0, \tag{24}$$

$$\frac{\partial H}{\partial t} = (U, V) \cdot \mathbf{n}_h, \tag{25}$$

$$\mathbf{t}_h \cdot \left(\frac{\partial U}{\partial Y} + \frac{\partial V}{\partial X} \right) \cdot \mathbf{n}_h = 0, \tag{26}$$

$$P = 0. \tag{27}$$

At $Y = S(X, \tau)$,

$$\theta = 0, \tag{28}$$

$$(\nabla\theta \cdot \mathbf{n}_s)_+ - K_{ls} (\nabla\theta \cdot \mathbf{n}_s)_- = \frac{\kappa}{St} \frac{\partial S}{\partial \tau}, \tag{29}$$

$$(U, V) \cdot \mathbf{t}_s = 0, \tag{30}$$

$$(1 - \rho) \frac{\partial S}{\partial \tau} = (U, V) \cdot \mathbf{n}_s, \tag{31}$$

where the Stefan number, St, is given by

$$St = \frac{c_{ps} (T_{hot} - T_{melt})}{\Delta H_f},$$

$K_{ls} = k_l / k_s$ and $\rho = \rho_s (T_{melt}) / \rho_l (T_{melt})$.

The initial conditions at $\tau = 0$ are, for $0 \le Y \le 1$,

$$\theta = 1, \quad U = 0, \quad V = 0, \tag{32}$$

and

$$S(X, 0) = 0, \tag{33}$$

$$H(X, 0) = 1. \tag{34}$$

THE LIMIT AS $\tau \to 0$

If $\rho = 1$, there will be an analytical (similarity) solution as $\tau \to 0$:

$$U = 0, \quad V = 0, \quad S = \lambda \tau^{1/2}, \quad H = 1,$$

$$\theta = \begin{cases} \theta_{cold} \left(1 - \frac{\operatorname{erf}\left(\kappa^{1/2}\eta/2\right)}{\operatorname{erf}\left(\lambda\kappa^{1/2}/2\right)} \right) & \text{if } Y < S(\tau) \\ 1 - \frac{\operatorname{erfc}(\eta/2)}{\operatorname{erfc}(\lambda/2)} & \text{if } Y > S(\tau) \end{cases} \tag{35}$$

where $\eta = Y/\tau^{1/2}$ and λ is a positive constant that is the solution to

$$-\kappa^{1/2}\theta_{cold} \frac{\exp\left(-\kappa\lambda^2/4\right)}{\operatorname{erf}\left(\lambda\kappa^{1/2}/2\right)} - K_{ls} \frac{\exp\left(-\lambda^2/4\right)}{\operatorname{erfc}(\lambda/2)} = \frac{\kappa\lambda\pi^{1/2}}{2St}; \tag{36}$$

equations (35) and (36) consitute the classical Neumann solution to the Stefan problem [10]. On the other hand, if $\rho \neq 1$, then (31), which becomes

$$(1 - \rho) \frac{\partial S}{\partial \tau} = V \tag{37}$$

in the limit as $\tau \to 0$, indicates that $V \neq 0$. Now, if $S \sim \tau^{1/2}$, we would need $V \sim \tau^{-1/2}$. Note that (19) then leads to $\partial V / \partial Y = 0$, giving at $V = V_0 \tau^{-1/2}$, where V_0 is a constant to be determined. Setting

$$U = 0, \quad P = P(Y, \tau),$$

equations (18)-(22) give

$$\kappa \frac{\partial \theta}{\partial \tau} = \frac{\partial^2 \theta}{\partial Y^2}, \tag{38}$$

$$\frac{1}{Pr} \left(\frac{\partial V}{\partial \tau} + V \frac{\partial V}{\partial Y} \right) = -\frac{\partial P}{\partial Y} + \frac{\partial^2 V}{\partial Y^2} + Ra\theta, \tag{39}$$

$$\frac{\partial \theta}{\partial \tau} + V \frac{\partial \theta}{\partial Y} = \frac{\partial^2 \theta}{\partial Y^2}; \tag{40}$$

note that equation (20) drops out, since the assumptions on U and P mean that it is satisfied exactly. The remaining boundary conditions are

$$\theta = \theta_{cold} \quad \text{at } Y = 0, \tag{41}$$

$$\theta = 0 \quad \text{at } Y = S(\tau), \tag{42}$$

$$\left(\frac{\partial \theta}{\partial Y} \right)_- - K_{ls} \left(\frac{\partial \theta}{\partial Y} \right)_+ = \frac{\kappa}{St} \frac{\partial S}{\partial \tau} \quad \text{at } Y = S(\tau), \tag{43}$$

$$V = (1 - \rho) \frac{\partial S}{\partial \tau} \quad \text{at } Y = S(\tau), \tag{44}$$

$$\frac{\partial \theta}{\partial Y} = 0 \quad \text{at } Y = H(\tau), \tag{45}$$

$$V = \frac{\partial H}{\partial \tau} \quad \text{at } Y = S(\tau); \tag{46}$$

the initial conditions are

$$\theta = 1, \quad V = 0, \quad 0 < Y < 1, \tag{47}$$

$$S(0) = 0, \tag{48}$$

$$H(0) = 1. \tag{49}$$

Now, we try

$$\theta = F_{s,l}(\eta, \tau), \quad V = V_0 \tau^{-1/2}, \quad P = \tau^{-1} \Pi(\eta, \tau),$$
$$S = \lambda \tau^{1/2}, \quad H = 1 + \nu\tau^{1/2}, \quad \eta = Y/\tau^{1/2}.$$

So, (38)-(40) become, in the limit as $\tau \to 0$,

$$-\frac{\kappa}{2} \eta \frac{dF_s}{d\eta} = \frac{d^2 F_s}{d\eta^2}, \tag{50}$$

$$-\frac{V_0}{2Pr} = -\frac{d\Pi}{d\eta}, \tag{51}$$

$$\left(V_0 - \frac{1}{2}\eta \right) \frac{dF_l}{d\eta} = \frac{d^2 F_l}{d\eta^2}, \tag{52}$$

subject to

$$F_s = \theta_{cold} \quad \text{at } \eta = 0, \tag{53}$$

$$F_l = 0 \quad \text{at } \eta = \lambda, \tag{54}$$

$$\frac{\partial F_s}{\partial \eta} - K_{ls} \frac{\partial F_l}{\partial \eta} = \frac{\lambda}{2} \left(\frac{\kappa}{St} \right) \quad \text{at } \eta = \lambda, \tag{55}$$

$$F_l \to 1 \quad \text{as } \eta \to \infty; \tag{56}$$

Parameter	Value
c_{pl}	4180 J kg^{-1} K^{-1}
c_{ps}	2217 J kg^{-1} K^{-1}
k_l	0.578 W m^{-1}K^{-1}
k_s	1.918 W m^{-1}K^{-1}
T_{melt}	273 K
ΔH_f	3.33×10^5 J kg^{-1}
$\rho_{l,0}$	1000 kg m^{-3}
ρ_s	918 kg m^{-3}

Table 1: Parameters for water

Parameter	Value
c_{pl}	495 J kg^{-1} K^{-1}
c_{ps}	485 J kg^{-1} K^{-1}
k_l	165 W m^{-1}K^{-1}
k_s	334 W m^{-1}K^{-1}
T_{melt}	1356 K
ΔH_f	2.05×10^5 J kg^{-1}
$\rho_{l,0}$	8000 kg m^{-3}
ρ_s	8900 kg m^{-3}

Table 2: Parameters for copper

note that equations (44) and (46) give

$$\nu = \lambda\,(1-\rho)\,, \quad V_0 = \frac{1}{2}\lambda\,(1-\rho)\,. \tag{57}$$

There is an analytical solution to F_s,

$$F_s = \theta_{cold}\left(1 - \frac{\operatorname{erf}\left(\eta\kappa^{1/2}/2\right)}{\operatorname{erf}\left(\lambda\kappa^{1/2}/2\right)}\right); \tag{58}$$

hence, F_l satisfies (52), subject to

$$F_l = 0 \quad \text{at } \eta = \lambda, \tag{59}$$

$$K_{ls}\frac{dF_l}{d\eta} = -\frac{\theta_{cold}\kappa^{1/2}\exp\left(-\kappa\lambda^2/4\right)}{\pi^{1/2}\operatorname{erf}\left(\lambda\kappa^{1/2}/2\right)} - \frac{\lambda\kappa}{2St} \quad \text{at } \eta = \lambda, \tag{60}$$

$$F_l \to 1 \quad \text{as } \eta \to \infty. \tag{61}$$

So, we arrive at

$$F_l = \frac{\operatorname{erf}\left(\frac{1}{2}\eta - V_0\right) - \operatorname{erf}\left(\frac{1}{2}\lambda - V_0\right)}{\operatorname{erfc}\left(\frac{1}{2}\lambda - V_0\right)}; \tag{62}$$

on using equation (60), we obtain a transcendental equation for λ,

$$-\frac{\kappa^{1/2}\theta_{cold}\exp\left(-\kappa\lambda^2/4\right)}{\operatorname{erf}\left(\lambda\kappa^{1/2}/2\right)} - \frac{K_{ls}\exp\left(-\lambda^2\rho^2/4\right)}{\operatorname{erfc}\left(\frac{1}{2}\lambda\rho\right)} = \frac{\lambda\kappa\pi^{1/2}}{2St}. \tag{63}$$

Once λ has been determined, $d\Pi/d\eta$ will also be fully determined.

There are several observations to make here. First of all, F_l, F_s, λ depend neither on Ra, nor on Pr, although Π does depend on Pr; furthermore, since the buoyancy term has dropped out of the system of equations, it means that the same equations will apply even for the case of freezing from above. Most alarmingly, we have found that $P \sim \tau^{-3/2}$.

RESULTS

We demonstrate these ideas for water and copper, for which $\rho < 1$ and $\rho > 1$, respectively. Defining

$$f\,(\lambda) := -\frac{\kappa^{1/2}\theta_{cold}\exp\left(-\kappa\lambda^2/4\right)}{\pi^{1/2}\operatorname{erf}\left(\lambda\kappa^{1/2}/2\right)} - \frac{K_{ls}\exp\left(-\lambda^2\rho^2/4\right)}{\pi^{1/2}\operatorname{erfc}\left(\frac{1}{2}\lambda\rho\right)} - \frac{\lambda\kappa}{2St}, \tag{64}$$

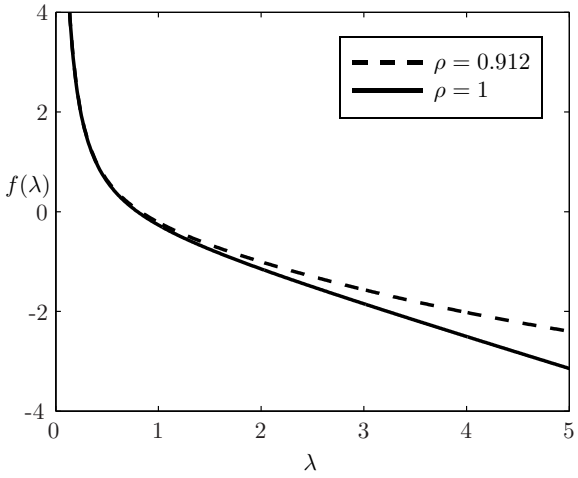

Figure 2: $f(\lambda)$ vs. λ for water

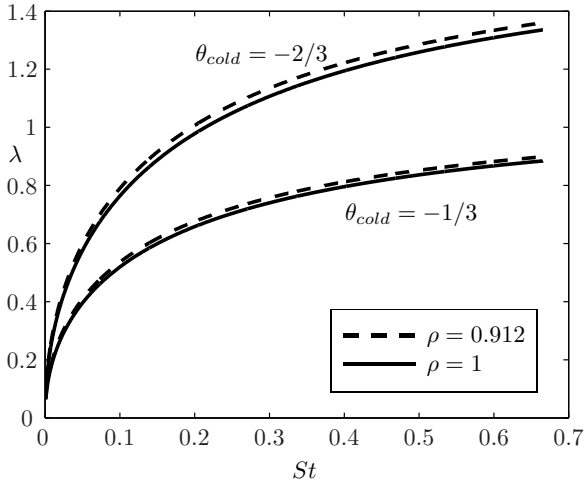

Figure 3: λ vs. St for water ($\theta_{cold} = -2/3, -1/3$)

Fig. 2 shows $f\,(\lambda)$ vs. λ using the parameters for ice and water, as given in Table 1; a comparison is made between $\rho = 1$ and the true value of $\rho = 0.912$. For this plot, we take $\theta_{cold} = -1/3$ and $St = 0.4$; in both cases, we would expect a unique positive solution for λ. Fig. 3 shows λ as a function of St for $\theta_{cold} = -2/3, -1/3$ and the two values

of ρ; this indicates that neglecting the density difference at $T = T_{melt}$ would underestimate the location of the front, although by considerably less than the 10% difference that there actually is in the densities.

Fig. 4 shows $f(\lambda)$ vs. λ using the parameters for solid and molten copper, as given in Table 2; a comparison is made between $\rho = 1$ and the true value of $\rho = 1.113$. For this plot, we also take $\theta_{cold} = -1/3$ and $St = 0.4$. Fig. 5 shows λ as a function of St for $\theta_{cold} = -2/3, -1/3$ and the two values of ρ; this indicates that neglecting the density difference at $T = T_{melt}$ would overestimate the location of the front, although once again by considerably less than the 10% difference that there actually is in the densities.

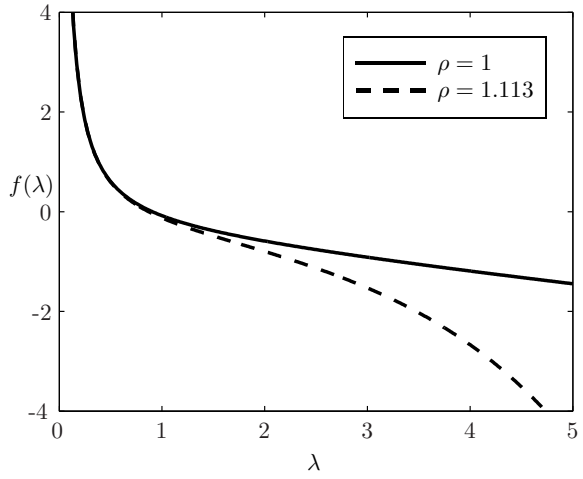

Figure 4: $f(\lambda)$ vs. λ for copper

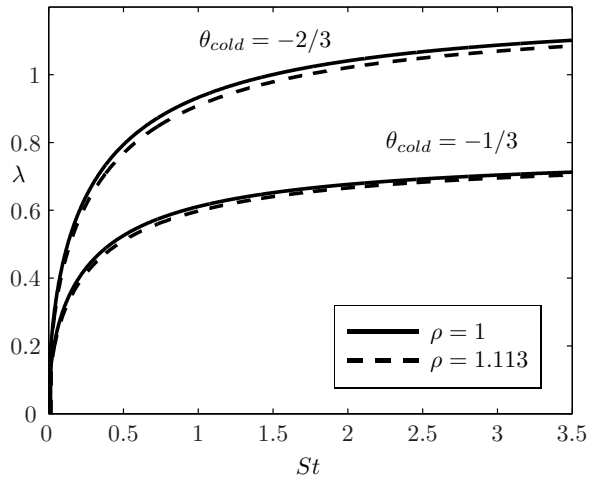

Figure 5: λ vs. St for copper ($\theta_{cold} = -2/3, -1/3$)

DISCUSSION

In addition to the singularity in the pressure as $\tau \to 0$, a further difficulty with the solution given above is that the solution obtained for V does not satisfy the initial condition (47). Consequently, the above analysis suggests that, inspite of the fact that Figs. 3 and 5 indicate that accounting for the solid/liquid density difference does not result in a particularly great difference in the prediction for the location of the solidification front, there are nevertheless considerable difficulties in obtaining a self-consistent description for initial heat and momentum transfer when considering cooling by means of an imposed temperature.

An alternative approach would then be to consider cooling by means of a different type of boundary condition. An obvious candidate is a heat-flux boundary condition; from an experimental point of view, this is also more realistic than a constant temperature condition. With this type of boundary condition, solidification will not begin immediately; instead, there will be a delay before phase change occurs. Some details of this case were given in [6], although the initial liquid region was assumed to be semi-infinite in extent and only a Neumann boundary condition was considered; here, the analysis is extended to a liquid of finite height and with cooling by means of a Robin boundary condition.

We replace (6) by

$$k_l \frac{\partial T}{\partial y} = \mathfrak{h}\left(T - T_{cold}\right), \tag{65}$$

where $\mathfrak{h}$ is a heat transfer coefficient and T_{cold} is a cooling temperature; for simplicity, both are assumed to be constant. Nondimensionalizing as before gives

$$\frac{\partial \theta}{\partial Y} = Bi\left(\theta - \theta_{cold}\right), \tag{66}$$

where $Bi\,(= h_0\mathfrak{h}/k_l)$ denotes the Biot number. Assuming the effects of natural convection to be weak to begin with, so that $U, V \approx 0$, we reduce (22) to

$$\frac{\partial \theta}{\partial \tau} = \frac{\partial^2 \theta}{\partial Y^2}, \tag{67}$$

which we solve subject to (24), (32) and (66); this gives

$$\theta\left(Y, \tau\right) = \hat{\theta}\left(Y, \tau\right) + \theta_{cold}, \tag{68}$$

where

$$\hat{\theta} = \sum_{n=1}^{\infty} B_n \left(\frac{\chi_n}{Bi}\cos\chi_n Y + \sin\chi_n Y\right)\exp\left(-\chi_n^2\tau\right), \tag{69}$$

with, for $n = 1, 2, ...,$

$$\chi_n \tan\chi_n = Bi \tag{70}$$

and

$$B_n = \frac{2\theta_{cold}}{\left(\frac{\chi_n^2}{Bi^2} + 1\right)\chi_n - \left(\frac{\chi_n^2}{Bi^2} - \frac{\chi_n}{Bi} - 1\right)\left(1 - \cos 2\chi_n\right)}. \tag{71}$$

Equation (68) solution holds until solidification starts; this will occur when $\theta = 0$ at $Y = 0$, i.e. when $\tau = \tau_m$, where τ_m satisfies

$$Bi\theta_{cold} + \sum_{n=1}^{\infty} B_n \chi_n \exp\left(-\chi_n^2\tau_m\right) = 0. \tag{72}$$

Now, we use the corresponding result from [6], which indicates that, when solidification starts,

$$S(\tau) \sim \lambda (\tau - \tau_m)^{3/2}, \tag{73}$$

where $\lambda = 4St\theta_{YY}(0, \tau_m)/3\pi^{1/2}$; hence, (68) gives

$$\lambda = -\frac{8St\theta_{cold}}{3Bi\pi^{1/2}} \times$$

$$\times \sum_{n=1}^{\infty} \frac{B_n \chi_n^3 \cos\chi_n Y \exp\left(-\chi_n^2 \tau\right)}{\left(\frac{\chi_n^2}{Bi^2} + 1\right)\chi_n - \left(\frac{\chi_n^2}{Bi^2} - \frac{\chi_n}{Bi} - 1\right)(1 - \cos 2\chi_n)}. \tag{74}$$

An interesting point here is that λ will not depend on ρ; as for $V(\tau)$, we will now have, from equation (44),

$$V(\tau) \sim \frac{3}{2}(1-\rho)\lambda(\tau - \tau_m)^{1/2}. \tag{75}$$

Furthermore, setting $P = \Pi(\eta, \tau)$, where $\eta = Y/(\tau - \tau_m)^{1/2}$, we obtain, from (51),

$$\frac{d\Pi}{d\eta} = -\frac{3}{4}(1-\rho)\lambda; \tag{76}$$

hence, the key points are that there is now no singularity in V, nor in P, when solidification starts, and equation (75) is consistent with the assumption that the liquid is initially stagnant.

It remains to speculate on what will happen if U, V are not negligible by the time solidification starts. In this case, it is unlikely that θ will be a function of Y alone, which suggests a particular point on $Y = 0$ will reach the freezing temperature before any other point. Consequently, it would be necessary to perform a two-dimensional analysis in order to determine the growth of the solidification front just after phase change begins; this is beyond the scope here, as it is a significantly more difficult task than the derivation of the one-dimensional analysis presented here.

CONCLUSIONS

This paper has considered the initial stages of solidification in the presence of natural convection when there is a difference in the solid and liquid densities at the freezing temperature. It was found the classical one-dimensional Stefan solution for the temperature fields in the solid and liquid phases results in a singularity in both the liquid pressure and velocity fields; this singularity is not present when the two densities are equal. Singularities can be avoided by not using a constant cooling-temperature boundary condition, but rather a heat flux condition. In this case, solidification does not begin instantaneously, but only after some finite time interval, t_m; thereafter, the solidification front moves as $(t - t_m)^{3/2}$, and the normal velocity of the liquid phase at the solidification front behaves as $(t - t_m)^{1/2}$. Although this appears to be an appealing resolution of the problem, a further difficulty will occur if convection has become significant before solidification starts; in this case, the advancing front will not be planar, but must originate from a point at the cooled boundary.

Although this paper has considered only the case of cooling and solidification from below, the analysis may also be of use in a corresponding analysis for solidification from above, as well as for problems involving melting.

ACKNOWLEDGMENTS

The author acknowledges the support of the Mathematics Applications Consortium for Science and Industry (www.macsi.ul.ie) funded by the Science Foundation Ireland Mathematics Initiative Grant 06/MI/005.

REFERENCES

[1] Gupta S. C., A moving grid numerical scheme for multi-dimensional solidification with transition temperature range, *Computer Methods in Applied Mechanics and Engineering*, Vol. 189, 2000, pp. 525-544

[2] Vynnycky M., and Kimura S., An analytical and numerical study of coupled transient natural convection and solidification in a rectangular enclosure, *International Journal of Heat and Mass Transfer*, Vol. 50, 2007, pp. 5204-5414

[3] Vynnycky M., and Kimura S., Towards a natural-convection model for the Mpemba effect, *Proceedings of the 19th International Symposium on Transport Phenomena, Reykjavik, Iceland, 17-20 August 2008*, Paper 216 (CD-ROM)

[4] Natale M. F., Marcus, E. A. S., and Tarzia D. A., Explicit solutions for one-dimensional two-phase free boundary problems with either shrinkage or expansion, *Nonlinear Analysis: Real World Applications*, Vol. 11, 2010, pp. 1946-1952

[5] Mitchell S. L., and Vynnycky M., Finite-difference methods with increased accuracy and correct initialization for one-dimensional Stefan problems, *Applied Mathematics and Computation*, Vol. 215, 2009, pp. 1609-1621

[6] Vynnycky M., and Mitchell, S. L., On the solution of Stefan problems with delayed onset of phase change, *Proceedings of the 7th International Conference on Heat Transfer, Fluid Mechanics and Thermodynamics, Antalya, Turkey, 19-21 July 2010,* pp. 709-714

[7] Davis S. H., Müller U., and Dietsche C., Pattern selection in single-component systems coupling Benard convection and solidification, *Journal of Fluid Mechanics*, Vol. 114, 1984, pp. 133-151

[8] Dietsche C., and Müller U., Influence of Benard convection on solid-liquid interfaces, *Journal of Fluid Mechanics,* Vol. 161, 1985, pp. 249-268

[9] Kumar P., Chakraborty S., Srinivasan K., and Dutta P., Rayleigh-Benard convection during solidification of an eutectic solution cooled from the top. *Metallurgical Material Transactions B*, Vol. 33B, 2002, pp. 605–612

[10] Carslaw H. S., and Jaeger J. C., Conduction of Heat in Solids, 2nd edition, Oxford University Press, 1959